

Synthesis of L-DOPA based pigments with different physic-chemical properties.

Koen P. Vercruysse^{1*}

¹Chemistry Department, Tennessee State University, Nashville, TN 37209

*Corresponding author: kvercruysse@tnstate.edu

Abstract Using air- or Fe²⁺/H₂O₂-mediated oxidation, the formation of melanin-like pigments from L-DOPA was evaluated. The effects of the various reaction conditions on the efficiency of the reaction and the physic-chemical properties of the pigments generated (UV-Vis absorbance, fluorescence emission) was evaluated. As previously observed for other phenolic and indolic compounds, the use of high concentrations of H₂O₂ resulted in melanin-like materials with a much lighter color. In addition, we observed that, unlike for air-mediated oxidation, the Fe²⁺/H₂O₂-mediated oxidation of L-DOPA can yield melanin-like pigmentation in an acidic environment. In general, our results suggest that depending on the intensity of the oxidizing reaction conditions involved, light- or dark-colored melanin-like pigments can be generated from L-DOPA. This may be an important factor when evaluating the visible outlook of histological specimens: the presence of a lighter color or the absence of a dark color may not necessarily mean the absence of melanin-like biomolecules. We discuss all our observations in the context of the importance of melanin-like pigmentation in human physiology.

Keywords: *melanin, L-DOPA, peroxide.*

1. Introduction

Melanins (MNs) are darkly colored pigments ubiquitously found in nature and excellent reviews regarding their biosynthesis, chemistry, classification and functions have been written.[1, 2] The precise chemical structure of the MNs is not firmly established. Based upon degradation reactions involving oxidation in an alkaline environment, various model structures have been proposed and it has been suggested that MNs should be described as “heterogenous polymers derived by the oxidation of phenols and subsequent polymerization of intermediate phenols and their resulting quinones”.[2] The main MN pigments found in mammalian cells are eumelanin and pheomelanin. Eumelanin is built from L-DOPA, an oxidation product of L-tyrosine and have a dark brown to black color. Pheomelanin is built from a combination of L-DOPA and L-cysteine and are typically reddish in color.[2]

MNs are found in melanocytes, stored in specialized organelles, the melanosome.[3] The formation of melanosomes is a complex, multi-stage process.[4] The biosynthesis and enzymology of MNs in melanocytes have been extensively studied and reviewed.[5] In this context the enzyme tyrosinase has received a lot of attention.[5] This enzyme is responsible for the first steps of the MN biosynthesis: the hydroxylation of L-tyrosine to L-

DOPA and subsequent oxidation to L-dopaquinone. In addition to tyrosinase, the premelanosome protein (PMEL, also known as PMEL17, SILV or gp100) has been discussed as an important contributor to the biosynthesis of MNs.[6] PMEL is an amyloid protein that forms a fibrous matrix inside early stage melanosomes upon which the pigment is deposited. Regulation of pH levels inside melanosomes is another important factor determining MN synthesis as the enzymatic or non-enzymatic formation of MNs from DOPA does not proceed in acidic environments. Proteins like two-pore channel 2 (TPC2) have been identified as important regulators of melanosome pH.[7] An additional class of MNs, the so-called neuromelanins (NMs), is built from L-DOPA or catecholamines like dopamine or norepinephrine.[2, 8, 9] NMs are considered an aberration from the normal metabolization pathways for these catecholamines and have been associated with oxidative stress conditions.[10-12]

Using L-DOPA or catecholamines as precursors, MNs can readily be synthesized in an alkaline environment in the presence of an oxidizing agent.[13-15] In previous reports we have presented our observations regarding the synthesis of MN-like pigments from a multitude of precursors using polysaccharides (PS) or a combination of Fe²⁺ and H₂O₂. [16-21] We observed that many PS can promote the formation of MN-like pigments using different types of precursors leading to darkly colored

solutions or materials. Despite the obvious presence of a darkly-colored pigment, the PS/pigment complexes tended to contain mostly PS material with very little pigment bonded to it as judged from FT-IR analyses.[20, 21] Using $\text{Fe}^{2+}/\text{H}_2\text{O}_2$ as the oxidizing combination, we generated MN-like pigments that in appearance could be light- or dark-colored, depending on the intensity of the oxidizing reaction conditions.[17, 18]

We have expanded these earlier observations by studying the synthesis of MN-like pigments from L-DOPA using air-oxidation in an alkaline environment or $\text{Fe}^{2+}/\text{H}_2\text{O}_2$ -mediated oxidation. The air-mediated oxidation of L-DOPA yielded darkly-colored materials when pH levels were above 6.0. The higher the pH of the reaction mixture, the more efficient the reaction appeared to be. The $\text{Fe}^{2+}/\text{H}_2\text{O}_2$ -mediated oxidation yielded light- or dark-colored pigments even under acidic conditions. The use of high concentrations of H_2O_2 resulted in melanin-like materials with a much lighter color.

2. Experimental Section

2.1. Materials

L-3,4-dihydroxyphenylalanine (L-DOPA) was obtained from Sigma-Aldrich (St Louis, MO). H_2O_2 solution at 3% (v/v) was obtained from Kroger Co (Cincinnati, OH) and used within one month of their purchase. $\text{FeCl}_2 \cdot 2\text{H}_2\text{O}$ and all other chemicals were obtained from Fisher Scientific (Waltham, MA). Fe^{2+} solutions were prepared in distilled water just prior to the start of the reactions.

2.2. Air-mediated synthesis of L-DOPA-based pigments

About 25mg L-DOPA was dispersed in 25mL distilled water, buffer (25mM phosphate, bicarbonate or acetate) or other solutions (25mM NaOH or 25mM NaOH mixed with HCl) with pH values ranging from 2.6 to 11.7 at room temperature (RT). At different time points, 500 μL aliquots from these mixtures were diluted with 500 μL distilled water and centrifuged. Aliquots (200 μL) of these centrifuged mixtures were placed in wells of a microplate for absorbance or fluorescence spectroscopy measurements or were diluted with 800 μL solvent for chromatographic analysis.

2.3. $\text{Fe}^{2+}/\text{H}_2\text{O}_2$ -mediated synthesis of L-DOPA-based pigments

In a first series of experiments, about 25mg L-DOPA was dispersed in 25mL aqueous mixtures containing 0.3mM Fe^{2+} and H_2O_2 with concentrations ranging between 0 and 1% v/v. In a second series of

experiments, about 25mg L-DOPA was dispersed in 25mL acetate buffer with pH values at 4.4, 3.8 or 3.1 and containing 0.3mM Fe^{2+} and 0.1% v/v H_2O_2 . All mixtures were kept at RT. At different time points, 500 μL aliquots from these mixtures were diluted with 500 μL distilled water and centrifuged. Aliquots (200 μL) of these centrifuged mixtures were placed in wells of a microplate for absorbance or fluorescence spectroscopy measurements or were diluted with 800 μL solvent for chromatographic analysis.

2.4. UV_Vis spectroscopy

UV/Vis spectroscopic measurements were made in wells of a 96-well microplate using the SynergyHT microplate reader from Biotek (Winooski, VT).

2.5. Fluorescence

Fluorescence measurements were made in wells of an opaque 96-well microplate using the SynergyHT microplate reader from Biotek (Winooski, VT) with excitation filter set at 360nm, emission filter set at 460nm and sensitivity factor set at 75.

2.6. Size exclusion chromatography (SEC)

SEC analyses were performed as described elsewhere.[22] The peak corresponding to L-DOPA was integrated for the signal at 275nm to determine the area-under-the-curve (AUC) as a measure of the concentration of L-DOPA present in the aliquots from the reaction mixtures.

2.7. FT-IR spectroscopy

FT-IR spectroscopic scans were made as described elsewhere.[22]

3. Results

3.1. Air-mediated synthesis of L-DOPA-based pigments

Fig.1 shows photographs taken of this experiment at various time points.

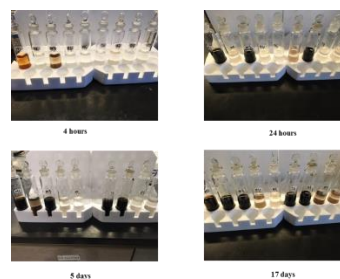


Fig.1: Photographs of 25mL mixtures containing 25mg DOPA in aqueous solutions at pH values = (from left to right) 11.7, 6.5, 9.1, 5.3, 2.6, 6.7, 7.85, 5.7 and distilled water; kept at RT for 4h, 24h, 5 days and 17 days.

The mixture at pH=11.7 immediately turned yellow-orange in color and was black in appearance within 24h of the start of the experiment. The mixtures at pH=7.85 and 9.1 had turned black in appearance as well within 24h, but this change in color progressed slower than the mixture at pH=11.7. Of all the other mixtures, only those with a pH value above 6.0 showed hints of a dark color after 24h of reaction. After five days of reaction, the mixture at pH = 6.7 had turned black in appearance, while the mixture at pH = 6.5 had significantly darkened in appearance. After 17 days of reactions the darkening of the mixtures with pH values above 6.5 had intensified. Fig.2 presents time profiles of the

changes in absorbance at 400nm (panel A), fluorescence emission (panel B) and % L-DOPA remaining (panel C) for the reaction mixtures in buffers with pH values at 11.7, 9.1, 7.85 or in distilled water. The % L-DOPA remaining was estimated by comparing the AUC corresponding to L-DOPA in any reaction mixture to the AUC corresponding to L-DOPA for the reaction mixture at pH = 2.6. The absolute value of the AUC corresponding to L-DOPA of that particular reaction mixture fluctuated without any particular pattern and for the four analyses performed during the course of the experiment the absolute value varied with a relative standard deviation of 5%.

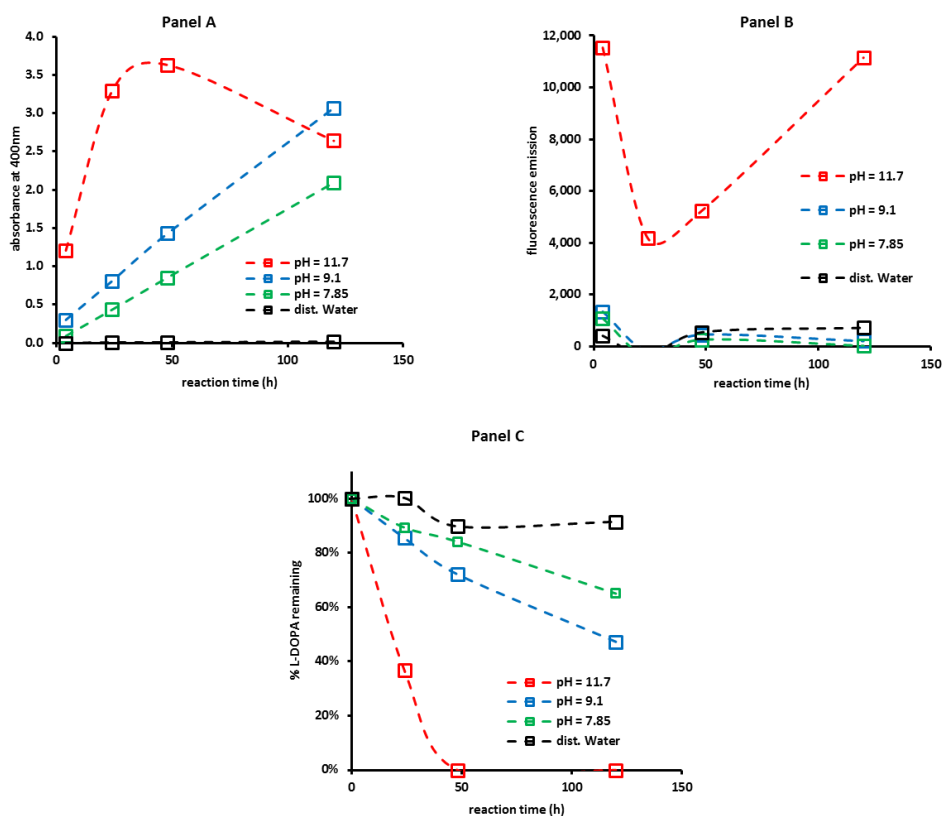


Fig.2: Kinetic profile of the changes in absorbance at 400nm (panel A), fluorescence emission (panel B) and % L-DOPA remaining (panel C) for 25mL reaction mixtures containing 25mg L-DOPA in buffers with pH values at 11.7, 9.1, 7.85 or in distilled water.

Fig.3 presents the SEC profiles of the reaction mixture at pH = 11.7 at various time points of the experiment. Panel A presents the SEC

chromatograms for the absorbance at 230nm, while panel B presents the UV-Vis spectra of the peak with retention time between 12.7 and 12.8 observed in these SEC profiles.

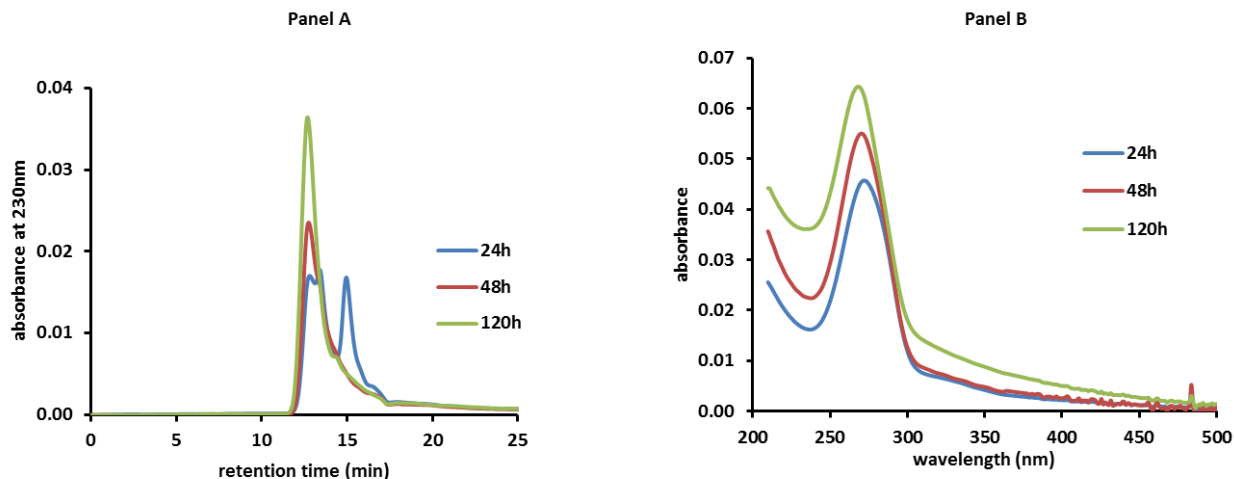


Fig. 3: SEC profiles (panel A) of a 25 mL reaction mixture containing 25mg L-DOPA in buffer with pH = 11.7 and the UV-Vis spectra (panel B) of the peak with retention time between 12.7 and 12.8 at various time points of the experiment.

Our observations and analyses are in line with the well-known fact that L-DOPA generates dark, MN-like pigments in non-acidic environments. However, it appears that very little reactivity was required to generate the appearance of dark pigment. The reaction mixture at pH = 7.85 looked black in appearance after 24h of reaction, but only 10% of L-DOPA had reacted away. In the reaction mixture at pH = 11.7, L-DOPA reacted away completely within 48h. In this mixture, the absorbance at 400nm increased rapidly within the first 24h, only to level off and decline. The kinetic profile of the fluorescence emission of this mixture exhibited an inverse pattern. The reaction mixtures at pH = 9.1 or 7.85 exhibited a linear increase of absorbance at 400nm as a function of reaction time; correlating with a steady decline in the % L-DOPA remaining. These mixtures exhibited no fluorescence emission.

SEC analyses of the reaction mixtures typically showed two peaks. A peak with retention time of about 15 minutes that corresponds to L-DOPA and a peak with retention time between 12.5 and 13 minutes. This latter peak corresponds to a high molecular mass material and the retention times were similar to the retention times observed for the formation of MN-like pigments from a wide range of other precursors.[17, 18, 23]. Figure 3, panel B, shows the UV-Vis spectra of the high molecular mass peak in the SEC chromatograms of the reaction mixture at pH = 11.7. The spectrum exhibits a prominent absorbance band with maximum around 270nm. Similar UV-Vis spectra were observed for the high molecular mass materials generated from L-DOPA in the reaction mixtures at pH = 9.1 or 7.85 (results not shown). The prominence of this peak appeared to decline with increasing reaction times

and the significance of all these observations is not clear at this moment.

3.2. $\text{Fe}^{2+}/\text{H}_2\text{O}_2$ -mediated synthesis of L-DOPA-based pigments

In a first series of experiments, the effect of the concentration of H_2O_2 on the pigment formation from L-DOPA was evaluated. Fig.4 shows photographs taken of this experiment at the start of the experiment and after three days of reaction at RT.

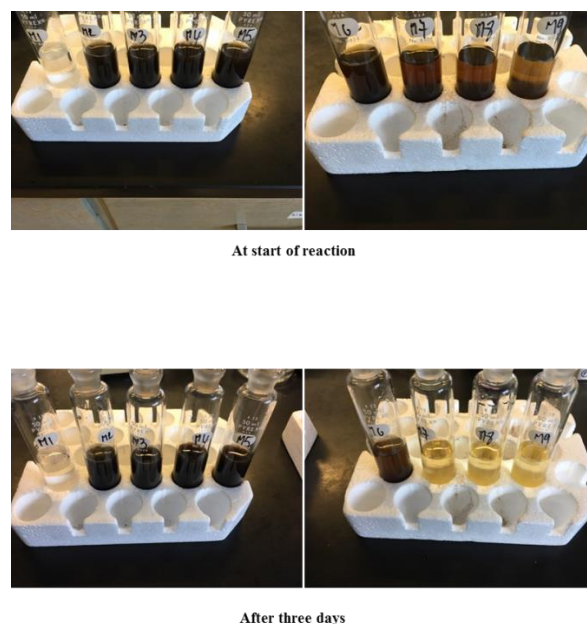


Fig. 4: Photographs of 25mL reaction mixtures containing 25mg L-DOPA, 0.3mM Fe^{2+} and, from left to right, 0, 0.01, 0.03, 0.06, 0.12, 0.24, 0.48, 0.72, 1.0% v/v H_2O_2 at the start of the experiment and after three days of reaction at RT.

All mixtures, except for the one without any H₂O₂, turned dark in color immediately upon the addition of H₂O₂. After three days, the mixtures containing the higher concentrations of H₂O₂ (0.48, 0.72 and 1.0 % v/v) had developed a much lighter color. The mixtures containing the lower concentrations of H₂O₂ (0.01, 0.03, 0.06 and 0.12 % v/v) had remained black in appearance. The mixture containing 0.24% v/v H₂O₂ had partially lightened up in color; having attained a brownish color. Fig. 5, panel A, presents

the absorbance at 400nm as a function of the concentration of H₂O₂ used in the reactions after 2.5h and three days of reaction. Fig. 5, panel B, presents the fluorescence emission as a function of the concentration of H₂O₂ used in the reactions after three days of reaction. Fig. 5, panel C illustrates some typical SEC profiles obtained for select reaction mixtures, while Fig 5, panel D, presents the UV-Vis spectra of the peaks with retention time between 12.7 and 12.8 observed in these SEC profiles.

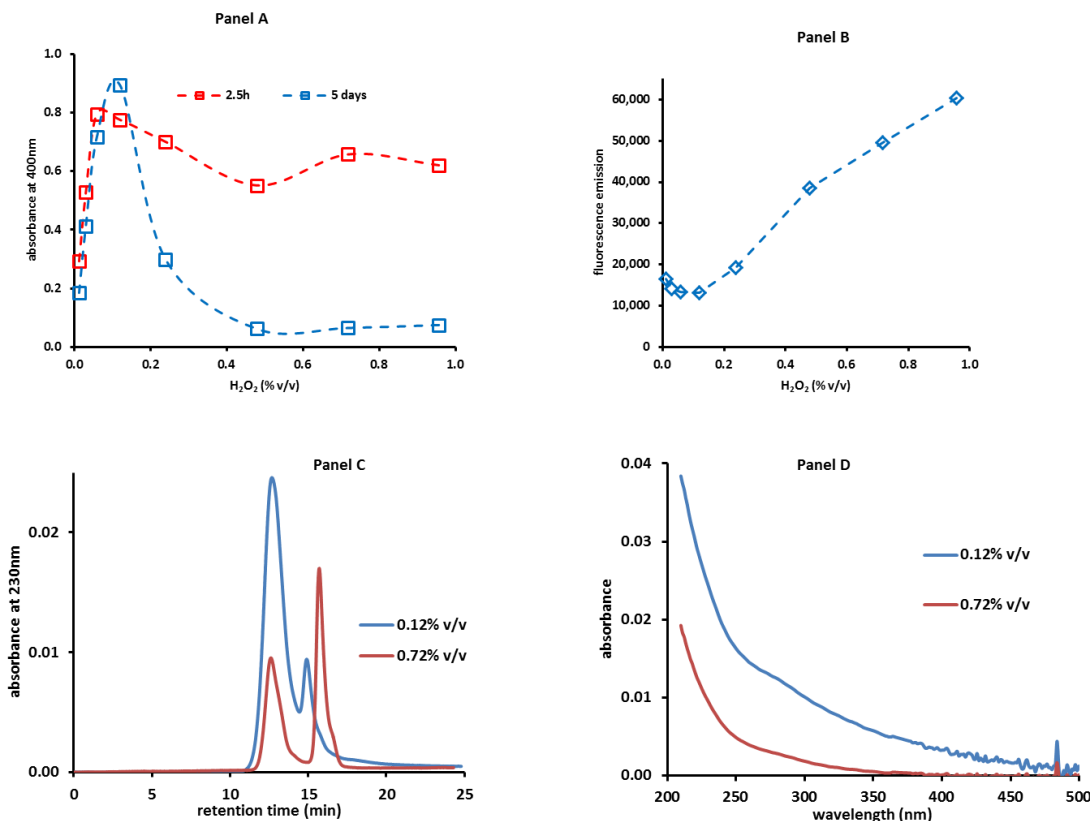


Fig. 5: Effect of H₂O₂ concentration in 25mL reaction mixtures containing 25mg L-DOPA and 0.3mM Fe²⁺ on the absorbance at 400nm (panel A) after 2.5h or three days of reaction and on the fluorescence emission (panel B) after three days of reaction. SEC profiles (panel C) and UV_Vis spectra (panel D) of the peaks with retention time between 12.7 and 12.8 observed in these SEC profiles of aliquots from reaction mixtures containing 0.12% or 0.72% v/v H₂O₂ after three days of reaction.

Fig. 5, panel A, illustrates the observation that, although all mixtures initially developed a dark color, those mixtures containing the higher concentrations of H₂O₂ developed a much lighter color later in the reaction. A pattern of results similar to what has been observed for the Fe²⁺/H₂O₂-mediated generation of MN-like pigments from a multitude of different precursors.[17] In addition, the results shown in Fig. 5, panel B, indicate that the pigments generated in the presence of higher concentrations of H₂O₂ exhibited enhanced fluorescence emissions. This pattern of observations is in line with what has been observed for MN-like pigments generated from other

precursors.[17, 18] The typical SEC profiles shown in Fig. 5, panel C, indicate peaks corresponding to high molecular mass materials (retention time about 12.8 minutes), unreacted L-DOPA (retention time about 15 minutes) and excess H₂O₂ (retention time about 16 minutes). The UV_Vis spectra corresponding to the high molecular mass peaks are shown in Fig. 5, panel D. They show the typical increasing absorbance with decreasing wavelength for MN-like pigments, with no prominent absorbance bands as seen in the materials generated through air-oxidation in an alkaline environment (see Fig. 3, panel B).

As the air-mediated oxidation of L-DOPA into MN requires pH values close to neutral or above, we briefly studied the effect of an acidic environment on the $\text{Fe}^{2+}/\text{H}_2\text{O}_2$ -mediated oxidation of L-DOPA as described in the section 2.3. Fig. 6 shows photographs taken of this experiment 1.5h and 48h after the start of the reaction.

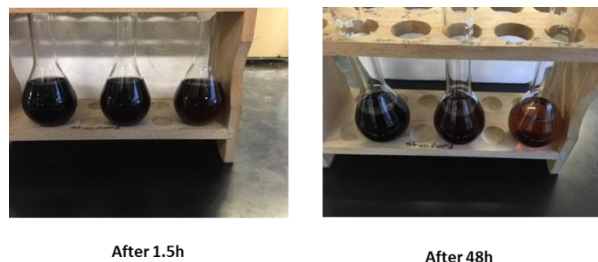


Fig. 6: Photographs after 1.5h and 48h of reaction of 25mL reaction mixtures containing 25mg L-DOPA, 0.3mM Fe^{2+} and 0.1% v/v H_2O_2 in 25mM acetate buffer with pH values at, from left to right, 4.4, 3.8 and 3.1 kept at RT.

Immediately upon the addition of H_2O_2 , the three mixtures turned a dark color. After 48h, the mixture at pH=3.1 appeared to have lightened up in color. Fig. 7 presents the absorbance at 400nm and the fluorescence emission of the mixtures as function of the pH after 48h of reaction.

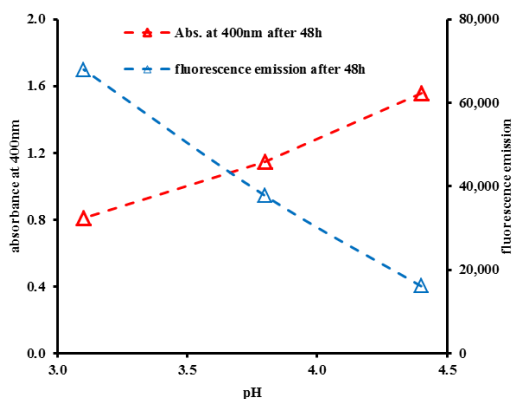


Fig. 7: Effect of pH on the absorbance at 400nm and fluorescence emission of 25mL reaction mixtures containing 25mg L-DOPA and 0.3mM Fe^{2+} and 0.1% v/v H_2O_2 after 48h of reaction at RT.

The results presented in Fig. 7 show a trend that the absorbance of the mixtures decreased with decreasing pH values (as reflected in the lighter color of the reaction mixture at pH = 3.1; see Fig. 6) and the fluorescence emission increased with decreasing pH values. SEC profiles and UV-Vis spectra of the peaks corresponding to the high molecular mass pigment materials of aliquots from these reaction mixtures were similar to those presented in Fig 5, panels C and D (results not shown).

4. Discussion

This report expands our earlier observations on the formation of MN-like pigments from a wide variety of catecholic or indolic precursors.[16-21, 23] The chemical processes used to generate these MN-like pigments are non-enzymatic, using air-mediated (in the presence of PS or alkaline solutions) or $\text{Fe}^{2+}/\text{H}_2\text{O}_2$ -mediated oxidation. Strong alkaline solutions are very effective in converting catecholic precursors like L-DOPA (this report), homogentisic acid[23], catechol or pyrogallol[17] into dark-colored, MN-like pigments. However, such reaction conditions are highly unlikely to be present under any *in vivo* conditions. When using milder levels of alkalinity, our current observations involving L-DOPA do indicate that, despite the fact that only minimal amounts of L-DOPA reacted away, the appearance of dark-colored solutions is readily obtained (see Fig. 1). A similar observation was made regarding the generation of MN-like pigments from a wide variety of precursors in the presence of PS.[16, 19-21] When using PS to generate MN-like pigments, dark-colored PS/pigment complexes were readily obtained. However, the FT-IR spectra of the PS/pigment complexes consistently contained the spectral features of the PS used in the reaction and no features of MNs. In the case of a PS/pigment complex synthesized from L-DOPA, the contribution of the pigment to the overall complex was estimated to be between 1.4 and 2.4% w/w and yet the PS/pigment complex was a darkly-colored substance.[21]

For the generation of MN-like pigments from various precursors through $\text{Fe}^{2+}/\text{H}_2\text{O}_2$ -mediated oxidation, the use of low concentrations of H_2O_2 leads to the appearance of dark-colored solutions (see Fig. 4) despite the fact that only minimal amounts of precursor reacts away as observed for L-DOPA in this report and for other compounds.[17] When using increasing concentrations of H_2O_2 the amount of precursor reacting away increases accordingly. Interestingly, the use of higher concentrations of H_2O_2 leads to the appearance of dark-colored solutions in the initial stage of the reaction followed by the lightening up of the colors as observed for L-DOPA in this report (see Fig. 4) and for other compounds.[17, 18] As for their dark-colored counterparts, these light-colored MN-like materials absorb or diffract light in the UV-range of the electromagnetic spectrum (see Fig. 5, panel D and [17, 18]), but markedly less in the visible range of the electromagnetic spectrum. In addition, the $\text{Fe}^{2+}/\text{H}_2\text{O}_2$ -mediated oxidation of L-DOPA can generate the appearance of dark solutions and MN-like materials

under acidic pH conditions as presented in this report (see Fig. 6).

Mild alkaline conditions and the presence of H_2O_2 can be expected *in vivo*. However, it is important to point out that none of the *in vitro* reaction conditions we explored to generate MN-like pigments are likely to be capable of generating the precursors to the MN pigments. Thus, enzymes like phenylalanine hydroxylase[24], tyrosinase[5], dopachrome tautomerase[25] or tryptophan hydroxylase[26] are necessary to generate the catecholic or indolic precursors from tyrosine or tryptophan. However, such enzymes may not be a necessity to generate the appearance of the typical dark colors associated with the presence of MN-like pigments. Non-enzymatic biomolecules like PS[16, 20, 21] can promote the oxidation of catecholic or indolic precursors into darkly-colored materials and the association of MN-like pigments with extracellular PS materials has been reported and discussed before.[27-29] Similarly, the amyloid-like protein Pmel17/Silver/gp100 is capable of generating MN-like pigments *in vitro* or *in vivo*. [6, 30, 31] Pmel17/Silver/gp100 is a melanocyte-specific protein within the matrix of the melanocytes upon which the MN pigment is deposited and organized.[32-34] It is worth noting that in the case of lignins, a plant-based polymeric substance derived from phenolic precursors, extracellular proteins containing so-called dirigent domains are involved in the deposition and organization of this pigment.[35-37]

Other reports have described the effects of H_2O_2 on the physical properties of MNs and detailed the loss of color or enhanced fluorescence.[38, 39] However, these reports involve the treatment of pre-formed MNs with H_2O_2 , while our work focuses on the use of H_2O_2 in the synthesis of MNs. In this and our previous reports[17, 18] we confirmed that the presence of high concentrations of H_2O_2 does lead to MN-like materials with decreased colored appearance and enhanced fluorescence emission. However, these physic-chemically different MN-like pigments do not appear to undergo any depolymerization as the SEC retention times of all the MN-like materials are very similar; independent of the reaction conditions that generated the pigments. Whether our observations have any relevance to any MN-related *in vivo* situations remains to be seen. However, it is worth pointing out that for greying of hair or vitiligo, conditions that are associated with the loss of pigmentation, the presence of increased levels of H_2O_2 has been discussed as a potential contributing factor to these changes in pigmentation.[40-42] In addition, the importance of H_2O_2 in the process of melanogenesis has been discussed before.[24] Our current and previous observations[17, 18] do suggest

a hypothesis that the absence of dark colors may not necessarily mean the absence of MN-like molecules, but could mean the presence of a different type of MN-like material. It is worth pointing out that the light-colored MN-like materials generated in the presence of high concentrations of H_2O_2 do absorb or scatter light in the UV range of the electromagnetic spectrum although to a less efficient extent than the dark-colored materials (see Figure 5, panel D and [17, 18]). These observations do suggest the possibility that protection from UV radiation, one of the main functions of MNs in physiology, does not necessarily require the presence of molecules that provide coloration. Our observations do also raise the hypothesis that any lack of anti-oxidant protection may lead to an increase in the presence of H_2O_2 or other reactive oxygen species possibly leading to the generation of lighter-colored MNs and giving the impression of a lack of MNs due to a lack of coloration. In this context it is worth pointing out that in the cases of vitiligo[43] or of ageing/greying hair[44] a reduced catalase activity was observed.

With regards to human physiology, the role of MNs to provide UV protection[45-48] and skin, hair or eye pigmentation[49, 50] has been and is still studied extensively. Such functions are not applicable to the so-called internal MNs.[51] NM present in certain brain areas is a typical example of an internal MN. NMs have been discussed as protective agents through their capacity to sequester transition metal ions, radical species or toxic organic molecules.[12, 52] Even the production of MN in skin cells has been discussed as a means to provide protection against genotoxic substances.[53] Alternatively, the capability to generate MN-like materials may be a means to neutralize and immobilize potentially toxic *o*-quinone oxidation products that may be generated from catecholamines under oxidative stress conditions.[9, 54] Similarly, ochronosis, the pigment synthesis associated with alkaptonuria, may be a means of sequestering and immobilizing excess homogentisic acid that may be damaging to chondrocytes.[55, 56]

Thus far, we have not yet explored the synthesis of pheomelanin-like pigments by including L-cysteine in our chemical reactions. As a wide variety of phenolic and indolic compounds can be turned into MN-like materials through the action of a wide variety of enzymatic and non-enzymatic reactions, the inclusion of L-cysteine in any of these reactions may further expand the physic-chemical complexity of the family of MN pigments. In addition, most studies focus on a single molecule, e.g., L-DOPA or dopamine, as the precursor of MNs. However, the fact that multiple different catecholic, e.g., L-DOPA, dopamine, norepinephrine, epinephrine or indolic,

e.g., serotonin, molecules may be present at the same time and location, it is conceivable that MN structures built from mixtures of different precursors may exist in some cells; particularly if non-enzymatic factors, e.g., the presence of ROS, are driving the MN synthesis. When studying the synthesis and the physical and chemical properties of MNs, it is worthwhile to branch out to the reports regarding other polyphenolic pigments like lignins (as discussed earlier) or tannins[57] as sufficient similarities exist regarding the chemistry and the discussion points between all these polyphenolic pigments derived from phenylalanine- or tyrosine-based precursors.

5. Acknowledgements

Dr. Verccruyse was in part supported by the Institute for Food, Agricultural and Environmental Research at Tennessee State University.

6. References

- [1] M. d'Ischia, K. Wakamatsu, F. Cicoira, E. Di Mauro, J.C. Garcia-Borrón, S. Commo, I. Galván, G. Ghanem, K. Kenzo, P. Meredith, A. Pezzella, C. Santato, T. Sarna, J.D. Simon, L. Zecca, F.A. Zucca, A. Napolitano, S. Ito, Melanins and melanogenesis: from pigment cells to human health and technological applications, *Pigment Cell Melanoma Res* 28(5) (2015) 520-44.
- [2] F. Solano, Melanins: Skin Pigments and Much More:Types, Structural Models, Biological Functions, and Formation Routes, *New Journal of Science* 2014 (2014) 28.
- [3] R.E. Boissy, M. Huizing, W.A. Gahl, Biogenesis of Melanosomes, *The Pigmentary System*, Blackwell Publishing Ltd 2007, pp. 155-170.
- [4] I.F.d.S. Videira, D.F.L. Moura, S. Magina, Mechanisms regulating melanogenesis(), *Anais brasileiros de dermatologia* 88(1) (2013) 76-83.
- [5] F. Solano, J.C. García-Borrón, *Enzymology of Melanin Formation, The Pigmentary System*, Blackwell Publishing Ltd 2007, pp. 261-281.
- [6] A.R. Hellstrom, B. Watt, S.S. Fard, D. Tenza, P. Mannstrom, K. Narfstrom, B. Ekestén, S. Ito, K. Wakamatsu, J. Larsson, M. Ulfendahl, K. Kullander, G. Raposo, S. Kerje, F. Hallbook, M.S. Marks, L. Andersson, Inactivation of Pmel alters melanosome shape but has only a subtle effect on visible pigmentation, *PLoS Genet* 7(9) (2011) e1002285.
- [7] A.L. Ambrosio, J.A. Boyle, A.E. Aradi, K.A. Christian, S.M. Di Pietro, TPC2 controls pigmentation by regulating melanosome pH and size, *Proceedings of the National Academy of Sciences* 113(20) (2016) 5622-5627.
- [8] P. Manini, L. Panzella, A. Napolitano, M. d'Ischia, Oxidation chemistry of norepinephrine: partitioning of the O-quinone between competing cyclization and chain breakdown pathways and their roles in melanin formation, *Chemical research in toxicology* 20(10) (2007) 1549-55.
- [9] A. Napolitano, P. Manini, M. d'Ischia, Oxidation chemistry of catecholamines and neuronal degeneration: an update, *Curr Med Chem* 18(12) (2011) 1832-45.
- [10] K. Wakamatsu, T. Murase, F.A. Zucca, L. Zecca, S. Ito, Biosynthetic pathway to neuromelanin and its aging process, *Pigment Cell Melanoma Res* 25(6) (2012) 792-803.
- [11] K. Wakamatsu, K. Tabuchi, M. Ojika, F.A. Zucca, L. Zecca, S. Ito, Norepinephrine and its metabolites are involved in the synthesis of neuromelanin derived from the locus coeruleus, *J Neurochem* (2015).
- [12] F.A. Zucca, E. Basso, F.A. Cupaioli, E. Ferrari, D. Sulzer, L. Casella, L. Zecca, Neuromelanin of the human substantia nigra: an update, *Neurotox Res* 25(1) (2014) 13-23.
- [13] E.S. Bronze-Uhle, J.V. Paulin, M. Piacenti-Silva, C. Battocchio, M.L.M. Rocco, C.F.d.O. Graeff, Melanin synthesis under oxygen pressure, *Polymer International* (2016) n/a-n/a.
- [14] S. Cho, S.-H. Kim, Hydroxide ion-mediated synthesis of monodisperse dopamine-melanin nanospheres, *Journal of Colloid and Interface Science* 458 (2015) 87-93.
- [15] C. Shillingford, C.W. Russell, I.B. Burgess, J. Aizenberg, Bioinspired Artificial Melanosomes As Colorimetric Indicators of Oxygen Exposure, *ACS Applied Materials & Interfaces* 8(7) (2016) 4314-4317.
- [16] K. Verccruyse, A. Clark, N. Alatas, D. Brooks, N. Hamza, M. Whalen, Polysaccharide-mediated synthesis of melanins from serotonin and other 5-hydroxy indoles, *bioRxiv* (2017).
- [17] K. Verccruyse, S. Russell, J. Knight, N. Stewart, N. Wilson, N. Richardson, Dark- or Light-Colored Melanins: Generating Pigments Using Fe²⁺ and H₂O₂, *chemRxiv* (2017).
- [18] K. Verccruyse, A. Taylor, J. Knight, Fe²⁺/H₂O₂-mediated oxidation of homogentisic acid indicates the production of ochronotic and non-ochronotic pigments. Implications in Alkaptonuria and beyond, *bioRxiv* (2017).
- [19] K. Verccruyse, L. Tyler, J. Readus, Gum Arabic promotes oxidation and ester hydrolysis, *bioRxiv* (2017).
- [20] K.P. Verccruyse, A.M. Clark, P.A.F. Bello, M. Alhumaidi, Using size exclusion chromatography to monitor the synthesis of melanins from catecholamines, *J Chromatogr B Analyt Technol Biomed Life Sci* 1061-1062 (2017) 11-16.
- [21] K.P. Verccruyse, T.S. Farris, M.M. Whalen, Interleukin-1 β and -6 release from immune cells by DOPA-based melanin as free pigment or complexed to carboxymethylcellulose, *bioRxiv* (2017).
- [22] K.P. Verccruyse, A.M. Clark, P.A.F. Bello, M. Alhumaidi, Using size exclusion chromatography to monitor the synthesis of melanins from catecholamines, *Journal of Chromatography B* 1061-1062 (2017) 11-16.
- [23] A.M. Taylor, K.P. Verccruyse, Analysis of Melanin-like Pigment Synthesized from Homogentisic Acid, with or without Tyrosine, and Its Implications in Alkaptonuria, *JIMD Rep* 35 (2017) 79-85.
- [24] K.U. Schallreuter, S. Kothari, B. Chavan, J.D. Spencer, Regulation of melanogenesis – controversies and new concepts, *Experimental Dermatology* 17(5) (2008) 395-404.
- [25] L. Guyonneau, F. Murisier, A. Rossier, A. Moulin, F. Beermann, Melanocytes and pigmentation are affected in dopachrome tautomerase knockout mice, *Molecular and cellular biology* 24(8) (2004) 3396-403.
- [26] L. Wang, H. Erlandsen, J. Haavik, P.M. Knappskog, R.C. Stevens, Three-Dimensional Structure of Human Tryptophan Hydroxylase and Its Implications for the Biosynthesis of the Neurotransmitters Serotonin and Melatonin, *Biochemistry* 41(42) (2002) 12569-12574.
- [27] M. d'Ischia, K. Wakamatsu, F. Cicoira, E. Di Mauro, J.C. Garcia-Borrón, S. Commo, I. Galván, G. Ghanem, K. Kenzo, P. Meredith, A. Pezzella, C. Santato, T. Sarna, J.D. Simon, L. Zecca, F.A. Zucca, A. Napolitano, S. Ito, Melanins and melanogenesis: from pigment cells to human health and technological applications, *Pigment Cell & Melanoma Research* 28(5) (2015) 520-544.

- [28] T. Kimura, W. Fukuda, T. Sanada, T. Imanaka, Characterization of water-soluble dark-brown pigment from Antarctic bacterium, *Lysobacter oligotrophicus*, *Journal of Bioscience and Bioengineering* 120(1) (2015) 58-61.
- [29] J. Zhong, S. Frases, H. Wang, A. Casadevall, R.E. Stark, Following Fungal Melanin Biosynthesis with Solid-State NMR: Biopolymer Molecular Structures and Possible Connections to Cell-Wall Polysaccharides, *Biochemistry* 47(16) (2008) 4701-4710.
- [30] A.K. Chakraborty, J.T. Platt, K.K. Kim, B.S. Kwon, D.C. Bennett, J.M. Pawelek, Polymerization of 5,6-dihydroxyindole-2-carboxylic acid to melanin by the pmel 17/silver locus protein, *Eur J Biochem* 236(1) (1996) 180-8.
- [31] Z.H. Lee, L. Hou, G. Moellmann, E. Kuklinska, K. Antol, M. Fraser, R. Halaban, B.S. Kwon, Characterization and subcellular localization of human Pmel 17/silver, a 110-kDa (pre)melanosomal membrane protein associated with 5,6-dihydroxyindole-2-carboxylic acid (DHICA) converting activity, *J Invest Dermatol* 106(4) (1996) 605-10.
- [32] C. Delevoye, F. Giordano, G. van Niel, G. Raposo, [Biogenesis of melanosomes - the chessboard of pigmentation], *Med Sci (Paris)* 27(2) (2011) 153-62.
- [33] A. Sitaram, M.S. Marks, Mechanisms of protein delivery to melanosomes in pigment cells, *Physiology (Bethesda)* 27(2) (2012) 85-99.
- [34] B. Watt, G. van Niel, G. Raposo, M.S. Marks, PMEL: a pigment cell-specific model for functional amyloid formation, *Pigment Cell Melanoma Res* 26(3) (2013) 300-15.
- [35] V. Burlat, M. Kwon, L.B. Davin, N.G. Lewis, Dirigent proteins and dirigent sites in lignifying tissues, *Phytochemistry* 57(6) (2001) 883-97.
- [36] L.B. Davin, N.G. Lewis, Lignin primary structures and dirigent sites, *Current Opinion in Biotechnology* 16(4) (2005) 407-415.
- [37] P.S. Hosmani, T. Kamiya, J. Danku, S. Naseer, N. Geldner, M.L. Guerinot, D.E. Salt, Dirigent domain-containing protein is part of the machinery required for formation of the lignin-based Casparian strip in the root, *Proceedings of the National Academy of Sciences* 110(35) (2013) 14498-14503.
- [38] W. Korytowski, T. Sarna, Bleaching of melanin pigments. Role of copper ions and hydrogen peroxide in autooxidation and photooxidation of synthetic dopa-melanin, *J Biol Chem* 265(21) (1990) 12410-6.
- [39] S. Kozikowski, L. Wolfram, R. Alfano, Fluorescence spectroscopy of eumelanins, *IEEE Journal of Quantum Electronics* 20(12) (1984) 1379-1382.
- [40] K.U. Schallreuter, P. Bahadoran, M. Picardo, A. Slominski, Y.E. Elasiuty, E.H. Kemp, C. Giachino, J.B. Liu, R.M. Luiten, T. Lambe, I.C. Le Poole, I. Dammak, H. Onay, M.A. Zmijewski, M.L. Dell'Anna, M.P. Zeegers, R.J. Cornall, R. Paus, J.P. Ortonne, W. Westerhof, Vitiligo pathogenesis: autoimmune disease, genetic defect, excessive reactive oxygen species, calcium imbalance, or what else?, *Exp Dermatol* 17(2) (2008) 139-40; discussion 141-60.
- [41] D.J. Tobin, Age-related hair pigment loss, *Curr Probl Dermatol* 47 (2015) 128-38.
- [42] J.M. Wood, H. Decker, H. Hartmann, B. Chavan, H. Rokos, J.D. Spencer, S. Hasse, M.J. Thornton, M. Shalhaf, R. Paus, K.U. Schallreuter, Senile hair graying: H₂O₂-mediated oxidative stress affects human hair color by blunting methionine sulfoxide repair, *FASEB J* 23(7) (2009) 2065-75.
- [43] K.U. Schallreuter, J.M. Wood, J. Berger, Low catalase levels in the epidermis of patients with vitiligo, *J Invest Dermatol* 97(6) (1991) 1081-5.
- [44] S. Kauser, G.E. Westgate, M.R. Green, D.J. Tobin, Human hair follicle and epidermal melanocytes exhibit striking differences in their aging profile which involves catalase, *J Invest Dermatol* 131(4) (2011) 979-82.
- [45] J. D'Orazio, S. Jarrett, A. Amaro-Ortiz, T. Scott, UV radiation and the skin, *Int J Mol Sci* 14(6) (2013) 12222-48.
- [46] A. Huijser, A. Pezzella, V. Sundstrom, Functionality of epidermal melanin pigments: current knowledge on UV-dissipative mechanisms and research perspectives, *Phys Chem Chem Phys* 13(20) (2011) 9119-27.
- [47] N. Maddodi, A. Jayanthi, V. Setaluri, Shining light on skin pigmentation: the darker and the brighter side of effects of UV radiation, *Photochem Photobiol* 88(5) (2012) 1075-82.
- [48] B. Marchetti, T.N.V. Karsili, Theoretical insights into the photo-protective mechanisms of natural biological sunscreens: building blocks of eumelanin and pheomelanin, *Physical Chemistry Chemical Physics* 18(5) (2016) 3644-3658.
- [49] N.G. Crawford, D.E. Kelly, M.E.B. Hansen, M.H. Beltrame, S. Fan, S.L. Bowman, E. Jewett, A. Ranciaro, S. Thompson, Y. Lo, S.P. Pfeifer, J.D. Jensen, M.C. Campbell, W. Beggs, F. Hormozdiari, S.W. Mpoloka, G.G. Mokone, T. Nyambo, D.W. Meskel, G. Belay, J. Haut, N.C.S. Program, H. Rothschild, L. Zon, Y. Zhou, M.A. Kovacs, M. Xu, T. Zhang, K. Bishop, J. Sinclair, C. Rivas, E. Elliot, J. Choi, S.A. Li, B. Hicks, S. Burgess, C. Abnet, D.E. Watkins-Chow, E. Oceana, Y.S. Song, E. Eskin, K.M. Brown, M.S. Marks, S.K. Loftus, W.J. Pavan, M. Yeager, S. Chanock, S.A. Tishkoff, Loci associated with skin pigmentation identified in African populations, *Science (New York, N.Y.)* 358(6365) (2017).
- [50] R.A. Sturm, D.L. Duffy, Human pigmentation genes under environmental selection, *Genome biology* 13(9) (2012) 248.
- [51] S. Dubey, A. Roulin, Evolutionary and biomedical consequences of internal melanins, *Pigment Cell Melanoma Res* 27(3) (2014) 327-38.
- [52] F.A. Zucca, J. Segura-Aguilar, E. Ferrari, P. Munoz, I. Paris, D. Sulzer, T. Sarna, L. Casella, L. Zecca, Interactions of iron, dopamine and neuromelanin pathways in brain aging and Parkinson's disease, *Prog Neurobiol* 155 (2017) 96-119.
- [53] I. Vasquez-Moctezuma, E. Mendez-Bolaina, D.J. Sanchez-Gonzalez, Skin detoxification cycles, *Indian J Dermatol Venereol Leprol* 78(4) (2012) 414-6.
- [54] F.D. Marco, C. Foppoli, R. Coccia, C. Blarmino, M. Perluigi, C. Cini, M.L. Marcante, Ectopic deposition of melanin pigments as detoxifying mechanism: a paradigm for basal nuclei pigmentation, *Biochemical and Biophysical Research Communications* 314(2) (2004) 631-637.
- [55] D. Braconi, L. Millucci, G. Bernardini, A. Santucci, Oxidative stress and mechanisms of ochronosis in alkaptonuria, *Free Radic Biol Med* 88(Pt A) (2015) 70-80.
- [56] J.B. Mistry, D.J. Jackson, M. Bukhari, A.M. Taylor, A role for interleukins in ochronosis in a chondrocyte in vitro model of alkaptonuria, *Clin Rheumatol* 35(7) (2016) 1849-56.
- [57] G. Carletti, G. Nervo, L. Cattivelli, Flavonoids and Melanins: A Common Strategy across Two Kingdoms, *International Journal of Biological Sciences* 10(10) (2014) 1159-1170.